NASA
Technical
Paper
2153

May 1983

Buckling and Failure Characteristics of Graphite-Polyimide Shear Panels

Mark J. Shuart and
Jane A. Hagaman

NASA

25th Anniversary
1958-1983

NASA Technical Paper 2153

1983

Buckling and Failure Characteristics of Graphite-Polyimide Shear Panels

Mark J. Shuart and
Jane A. Hagaman
Langley Research Center
Hampton, Virginia

National Aeronautics
and Space Administration

**Scientific and Technical
Information Branch**

Use of trade names or names of manufacturers in this report does not constitute an official endorsement of such products or manufacturers, either expressed or implied, by the National Aeronautics and Space Administration.

SUMMARY

The buckling and failure characteristics of unstiffened, blade-stiffened, and hat-stiffened graphite-polyimide shear panels are described. The picture frame shear test is used to obtain shear stress-strain data at room temperature and at 316°C. The experimental results are compared with a linear buckling analysis, and the specimen failure modes are described. The effect of the 316°C test temperature on panel behavior is discussed. Significant postbuckling shear strength was observed for the unstiffened specimens. For all specimens, failure was caused by either a fixture-induced instability or by the stiffeners debonding from the skin.

INTRODUCTION

Graphite-polyimide composites have the same strength and stiffness advantages of graphite-epoxy composites and have a greater working temperature range than any currently available epoxy matrix system. One particular application for a high-temperature, low-weight material is the aft body flap of the Space Shuttle (fig. 1). This paper describes a preliminary study of the buckling and failure characteristics of graphite-polyimide shear panels tested at room temperature and at an elevated temperature typical of the service environment for the Shuttle aft body flap.

The picture frame shear test has been used to obtain shear stress-strain data for several composite structures (refs. 1 to 3). Although severe stress concentrations are developed in the specimen corners and in the regions of load introduction, the test is simple to use and results in a uniform shear stress state in the center of the test specimen.

In this study, the shear stress-strain behavior of unstiffened, blade-stiffened, and hat-stiffened graphite-polyimide panels at both room temperature and 316°C are examined. A finite-element analysis is used to calculate the initial buckling loads for each panel configuration. Also, the panel failure modes are described. Finally, effects of a 316°C temperature on panel behavior are discussed.

SYMBOLS

G_{xy} inplane shear modulus, GPa

N_{xy} shear stress resultant, kN/m

$(N_{xy})_{critical}$ shear stress resultant at buckling, kN/m

$(N_{xy})_{failure}$ shear stress resultant at failure, kN/m

P applied load, kN

RT room temperature

γ_{xy} shear strain

$(\gamma_{xy})_{critical}$ shear strain at buckling

$(\gamma_{xy})_{failure}$ shear strain at failure

$\varepsilon_1, \varepsilon_2$ measured strain

Subscript:

s symmetric

EXPERIMENTAL INVESTIGATION

This section describes the test specimens and the experimental procedure used in this study. The materials used in fabrication and the specimen geometry are described. The procedures for the tests conducted at room temperature and at 316°C are discussed.

Specimens

Panels were fabricated with either Celion[1] 6000/PMR-15 (0.13 to 0.16 mm per ply) or Celion 3000/PMR-15 (0.08 mm per ply) graphite-polyimide preimpregnated tape and typical specimens are shown in figure 2. All specimens had stainless-steel reinforcements secondarily bonded to the edges of the composite skin to help introduce loads into the panels. Stiffeners were also secondarily bonded to the skin. EA 934[2] and FM-34[3] adhesives were used for the room-temperature and the 316°C tests, respectively. All specimens were nominally 0.51 m long by 0.36 m wide, and details of the specimen cross-sections are shown in figure 3.

Experimental Procedure

Each specimen was bolted to a stainless-steel picture-frame test fixture at room temperature and tested in a hydraulic test machine. The specimen-fixture assembly was loaded through diagonally opposite corners in tension. A typical specimen in the test fixture is shown in figure 4 prior to testing. Quartz lamps were used to heat the specimens to 316°C, and the lamps, fixture, and specimen were surrounded by glass cloth to minimize any effects of air currents. Upon reaching 316°C, the specimen and fixture were heated for an additional 15 to 20 minutes to achieve thermal equilibrium. Thermocouples at various locations on the specimen recorded the specimen temperature, and the temperature variation in the test section was no more than ±5°C. Electrical resistance strain-gage rosettes were used to measure strain data, and changes in gage resistance due to temperature were accounted for during data reduction. Unstiffened panels had back-to-back rosettes at several locations; however, back-to-back rosettes were not used on the stiffened panels.

For tests at room temperature, the moiré-fringe technique was used to monitor out-of-plane deflections. A typical moiré-fringe pattern of the skin buckling mode

---

[1]Celion: product of Celion Corporation.
[2]EA 934: product of Hysol Division, The Dexter Corporation.
[3]FM-34: product of American Cyanamid Company.

prior to failure is shown in figure 5. The moiré-fringe technique was not used for the elevated temperature tests.

RESULTS AND DISCUSSION

Shear stress resultant and shear strain data are described in this section. Experimental and analytical buckling data and the differences between results obtained at room temperature and at 316°C are discussed. Failure data are also discussed, and the failure modes are described.

Buckling Results

Experimental data.- Buckling data for the unstiffened panels are given in table 1. The point at which buckling occurred was determined by the data from back-to-back strain gages on the panel. The applied load was plotted as a function of membrane strain, and the load at the initial change in the slope of the applied-load—membrane-strain curve was used to define the buckling load (e.g., fig. 6). Scatter in the buckling data may have been due to initial imperfections in the specimens. Since strain gages were applied to only one side of the stiffened panels, experimental buckling data were not obtained for these specimens.

Analytical results.- A linear, elastic finite-element analysis was performed to predict buckling loads and mode shapes for each specimen configuration. The composite specimen and the metal test fixture were discretely modeled and were mathematically connected at coincident finite-element nodes. Material properties were obtained from references 4 to 6, and the properties were assumed to be independent of test temperature.

Predicted buckling results from the finite-element models for all panel configurations are given in table 2. The predicted global inplane shear moduli are also given for comparison. The blade-stiffened configuration had the highest shear stress resultant at buckling for the specimens studied at both test temperatures because it had the thickest skin (fig. 3). Also, significant differences between data at room temperature and at 316°C for each specimen configuration were observed because of the mismatch of coefficients of thermal expansion between the composite panel and the metal fixture. The coefficient of thermal expansion for stainless steel is more than four times that for quasi-isotropic graphite-polyimide laminates. This mismatch induces thermal stresses in the test specimens that cause the predicted buckling results at 316°C to be considerably lower than those at room temperature.

In addition to the thermal stress state due to the coefficient of thermal expansion mismatch, the response of the hat-stiffened panels tested at 316°C was affected by convection heat transfer inside the stiffeners. Because a hat stiffener is a closed-section stiffener, only the outside surface of each stiffener could be heated. The inside surface of each stiffener remained cooler than the outside surface since heat was convected away by air currents inside the stiffener. In this buckling analysis, the temperature gradient through the stiffener walls was assumed to be linear. The analysis showed that this gradient contributed to the lower buckling data for the tests at 316°C.

Buckling mode shapes.- The analysis also predicted the mode shapes for each panel at buckling. The predicted results at room temperature are discussed first. For the unstiffened panels, the analysis predicted two half-waves for the lowest

buckling mode (fig. 7), which agrees with experiment as shown in figure 5 (the buckling mode shape did not change during the test). The analysis predicted a blade-rolling mode for the blade-stiffened panel and a local or short wavelength buckling mode in the unstiffened region (fig. 8) between the reinforcements and the start of the stiffened skin for the hat-stiffened panel.

The predicted mode shapes at 316°C were also determined. The unstiffened and blade-stiffened panels had global buckling modes of one half-wave and five half-waves, respectively, oriented similar to the mode shape for the unstiffened panel tested at room temperature. The hat-stiffened panel buckled into the same mode at 316°C as at room temperature.

Comparison of experimental and analytical results.- Typical data for shear stress resultant plotted against shear strain for unstiffened, blade-stiffened, and hat-stiffened panels are shown in figures 9, 10, and 11, respectively. Predicted buckling results are also shown in the figures. For all panels, the initial slope of the experimental curve agrees with the linear analysis. For the unstiffened panels, the room-temperature buckling data and analytical results (tables 1 and 2) agree. Differences between experimental and analytical results for the tests at 316°C may have been because of the thermal stress state at this temperature caused by the mismatch of coefficients of thermal expansion (see section "Analytical results"). For the hat-stiffened panels, the difference between room-temperature and 316°C results (fig. 11) may be attributed to the nonuniform temperature distribution caused by convection heat transfer discussed previously.

Failure Results

Shear stress resultants and shear strains at failure are given in table 3 for all specimen configurations. For all configurations, the shear stress resultant at failure was higher than that at buckling. For the unstiffened panels tested at room temperature and for all panels tested at 316°C, the buckling and failure loads were approximately an order of magnitude or more apart indicating significant postbuckling shear strength. As discussed in this section, the failure modes were affected by the test technique; hence, the data in table 3 represent a lower bound on the panel shear strengths.

The mechanism of failure of the unstiffened panels was a fixture-initiated instability and is illustrated in figure 12. Because of specimen geometry and loading, a strip in the specimen center was equivalently loaded in compression. Failure occurred when this strip buckled because of the inplane compressive loading. For the room-temperature tests, the calculated buckling load for this strip (ref. 7) was within the scatter of the specimen failure loads. Failed unstiffened test specimens are shown in figure 13. Figure 13(a) shows a failure in the specimen corner at the reinforcement-skin interface which is a region of severe stress concentrations. Figure 13(b) shows a similar failure for a specimen tested at 316°C. The failure data obtained at 316°C were lower than those obtained at room temperature (table 3). This difference in failure results may be because of the different adhesives used for specimen fabrication. The reinforcements disbonded from the skin at elevated temperature (fig. 13(b)) which increased the width of the strip in compression. An increase in strip width of 10 to 20 mm (depending on the degree of disbonding) would result in strip buckling loads within the scatter of the failure loads for specimens tested at 316°C.

The failure mechanism for the stiffened panels is shown in figure 14. As a result of the buckling modes, significant inplane and out-of-plane stresses caused the stiffeners to disbond as illustrated in figure 14(b). This failure mechanism was independent of test temperature. Again, the differences between the stiffened panel data obtained at room temperature and at 316°C may be due to the different adhesives used.

CONCLUDING REMARKS

The buckling and failure characteristics of unstiffened, blade-stiffened, and hat-stiffened graphite-polyimide shear panels were examined at room temperature and at 316°C. For the configurations studied, the blade-stiffened panel had the highest predicted buckling shear stress resultant at both test temperatures because it had the thickest skin. Also, for all configurations, thermal stresses caused the predicted buckling results at 316°C to be considerably lower than those at room temperature. For the unstiffened specimens, failure occurred at loads approximately an order of magnitude greater than the initial buckling load indicating significant postbuckling shear strength, and the failure was due to a fixture-induced instability. Failure of all the stiffened panels was initiated by the stiffeners debonding from the skins.

Langley Research Center
National Aeronautics and Space Administration
Hampton, VA 23665
March 23, 1983

REFERENCES

1. Ashton, J. E.; and Love, T. S.: Shear Stability of Laminated Anisotropic Plates. Composite Materials: Testing and Design, ASTM STP 460, 1969, pp. 352-361.

2. Kaminski, B. E.; and Ashton, J. E.: Diagonal Tension Behavior of Boron-Epoxy Shear Panels. J. Compos. Mater., vol. 5, Oct. 1971, pp. 553-558.

3. Davis, Randall C.: Stress Analysis and Buckling of J-Stiffened Graphite-Epoxy Panel. NASA TP-1607, 1980.

4. Argon, Ali S.; Backer, Stanley; McClintock, Frank A.; Reichenbach, George S.; Orowan, Egon; Shaw, Milton C.; and Rabinowicz, Ernest: Mechanical Behavior of Materials. Addison-Wesley Pub. Co., Inc., c.1966.

5. Farley, Gary L.: Effects of Static Tensile Load on the Thermal Expansion of Gr/PI Composite Materials. NASA TP-1867, AVRADCOM TR 81-B-2, 1981.

6. Cushman, J. B.; and McCleskey, S. F.: Design Allowables Test Program, Celion 3000/PMR-15 and Celion 6000/PMR-15, Graphite/Polyimide Composites. NASA CR-165840, 1982.

7. Timoshenko, Stephen P.; and Gere, James M.: Theory of Elastic Stability, Second ed. McGraw-Hill Book Co., 1961.

TABLE 1.- EXPERIMENTAL BUCKLING DATA FOR UNSTIFFENED PANELS

Specimen	Test temperature, °C	$(\gamma_{xy})_{critical}$	$(N_{xy})_{critical}$, kN/m
1	RT	0.00025	4.59
2	RT	.00016	3.94
3	RT	.00026	4.73
4	316	.00008	1.26
5	316	.00005	1.22
6	316	.00005	1.15

TABLE 2.- PREDICTED SHEAR MODULUS, STRAIN, AND STRESS RESULTANT AT BUCKLING

Specimen configuration	Test temperature, °C	G_{xy}, GPa	$(\gamma_{xy})_{critical}$	$(N_{xy})_{critical}$, kN/m
Unstiffened	RT	21.4	0.00020	4.9
	316		.00008	2.0
Blade stiffened	RT	24.3	.00385	135.6
	316		.00016	5.6
Hat stiffened	RT	24.3	.00161	48.0
	316		.00010	3.0

TABLE 3.- PANEL FAILURE DATA

Specimen configuration	Test temperature, °C	$(\gamma_{xy})_{failure}$	$(N_{xy})_{failure}$, kN/m
Unstiffened	RT	0.0024	44.7
	RT	.0022	44.0
	RT	.0022	38.9
	316	.0015	30.3
	316	.0007	15.9
	316	.0016	21.5
Blade stiffened	RT	.0068	194.6
	RT	.0072	201.4
	RT	.0054	174.1
	316	.0106	301.6
	316	.0076	240.1
Hat stiffened	RT	.0048	65.1
	RT	.0032	76.7
	RT	.0016	49.7
	316	.0027	72.7
	316	.0044	84.9
	316	.0047	79.9

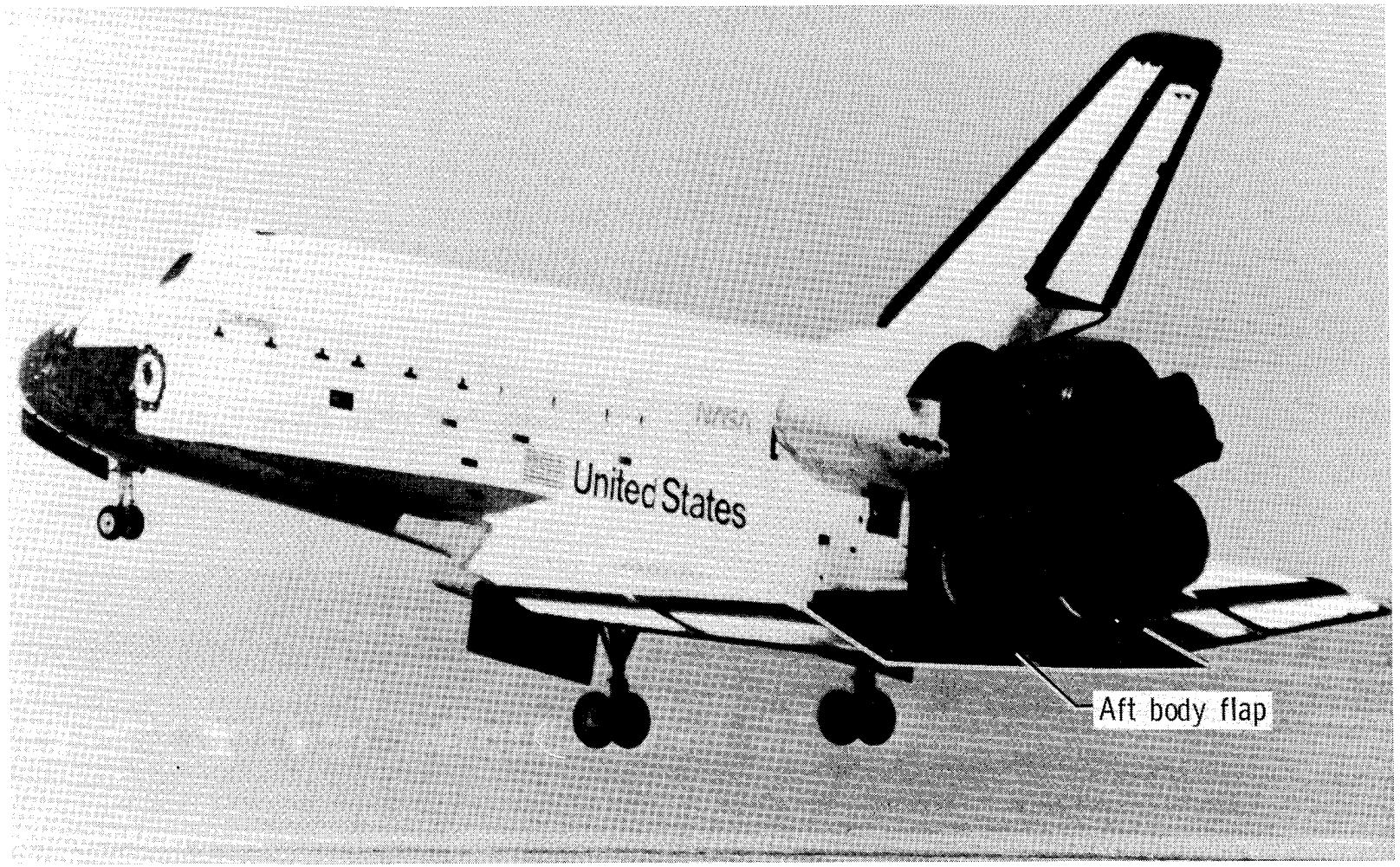

L-81-4378.1

Figure 1.- Aft body flap on Space Shuttle.

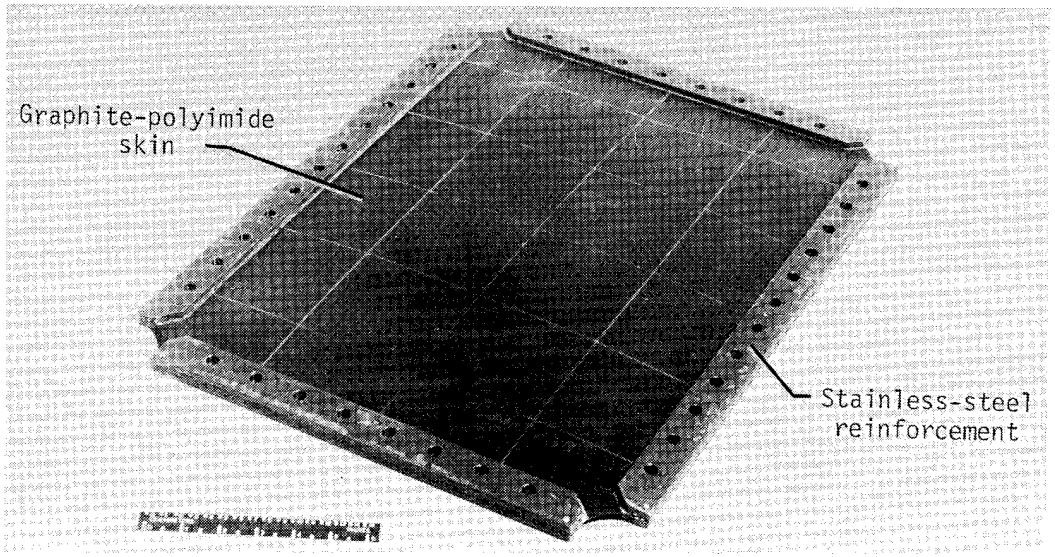

(a) Unstiffened panel.

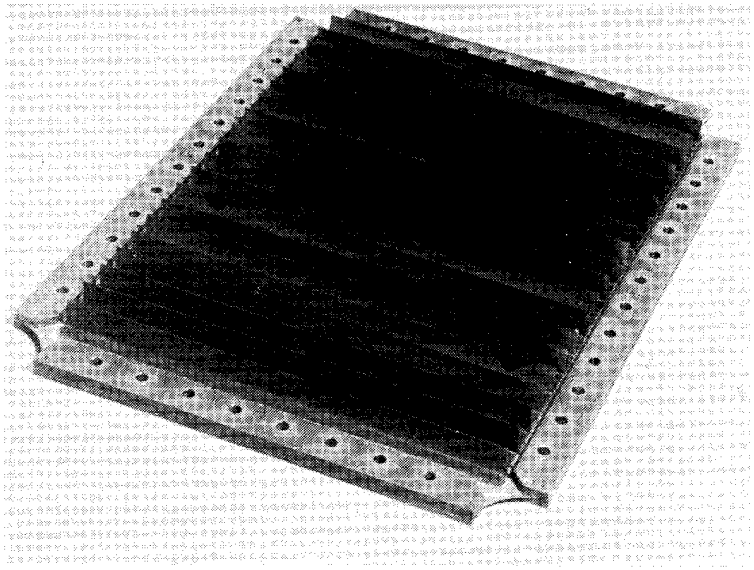

(b) Blade-stiffened panel.

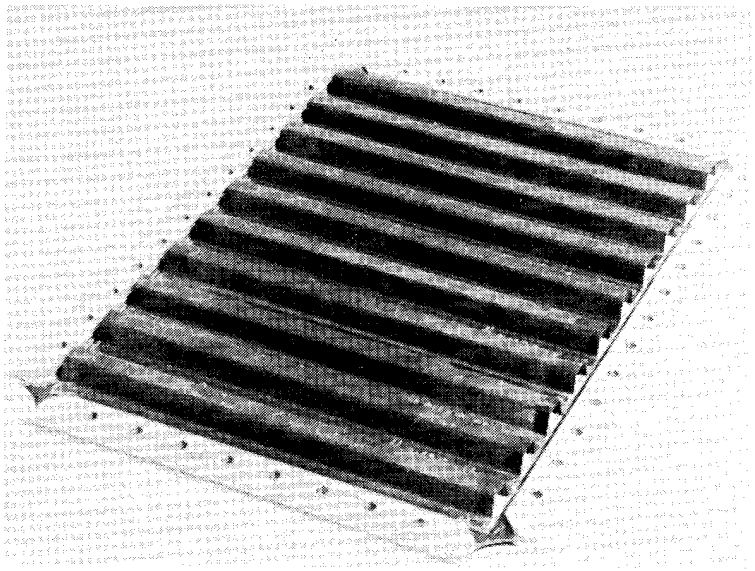

(c) Hat-stiffened panel.

L-83-52

Figure 2.- Typical test specimens.

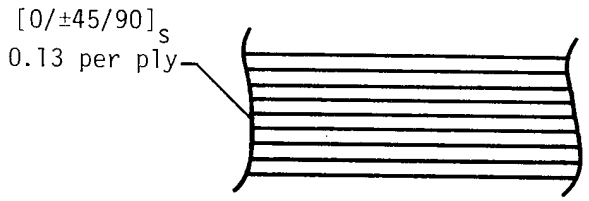

(a) Unstiffened panel.

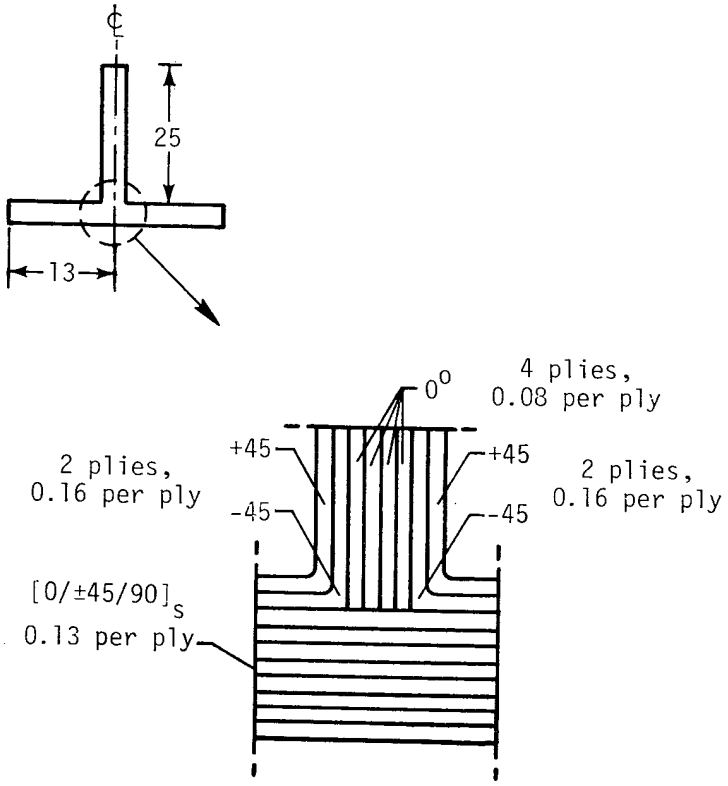

(b) Repeating element for blade-stiffened panel.

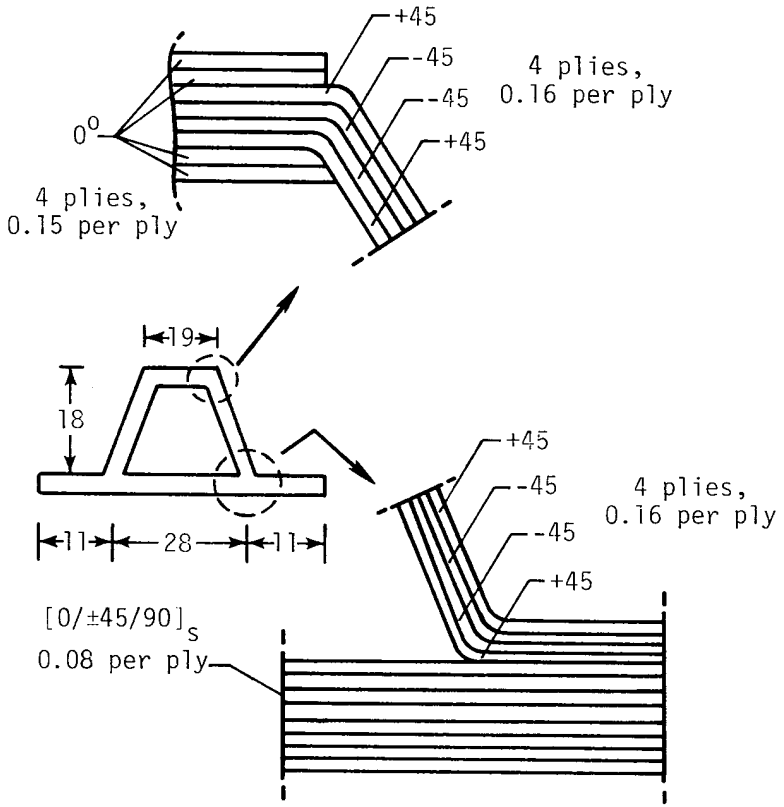

(c) Repeating element for hat-stiffened panel.

Figure 3.- Panel cross-section geometries. All dimensions are in millimeters.

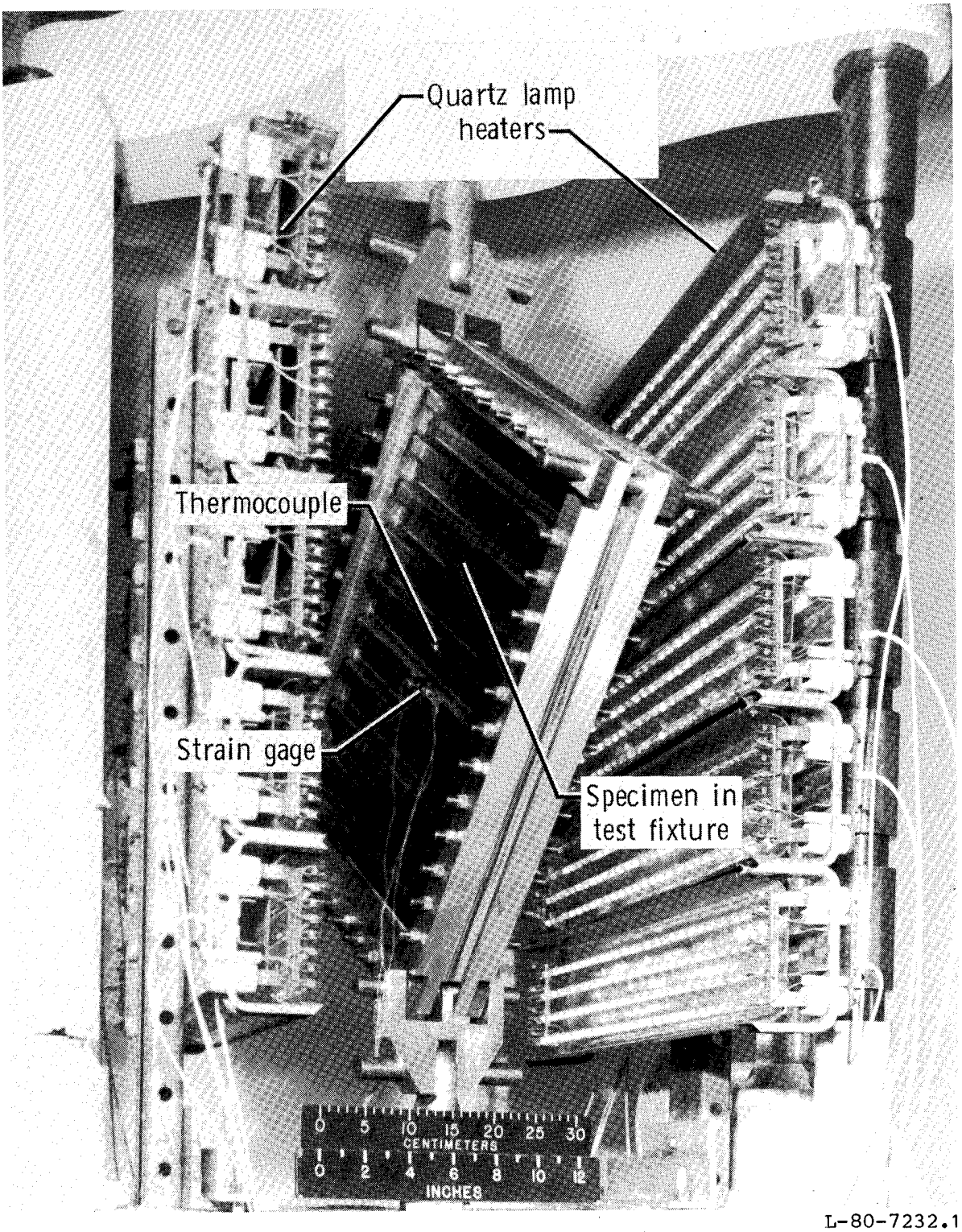

L-80-7232.1

Figure 4.- Test apparatus.

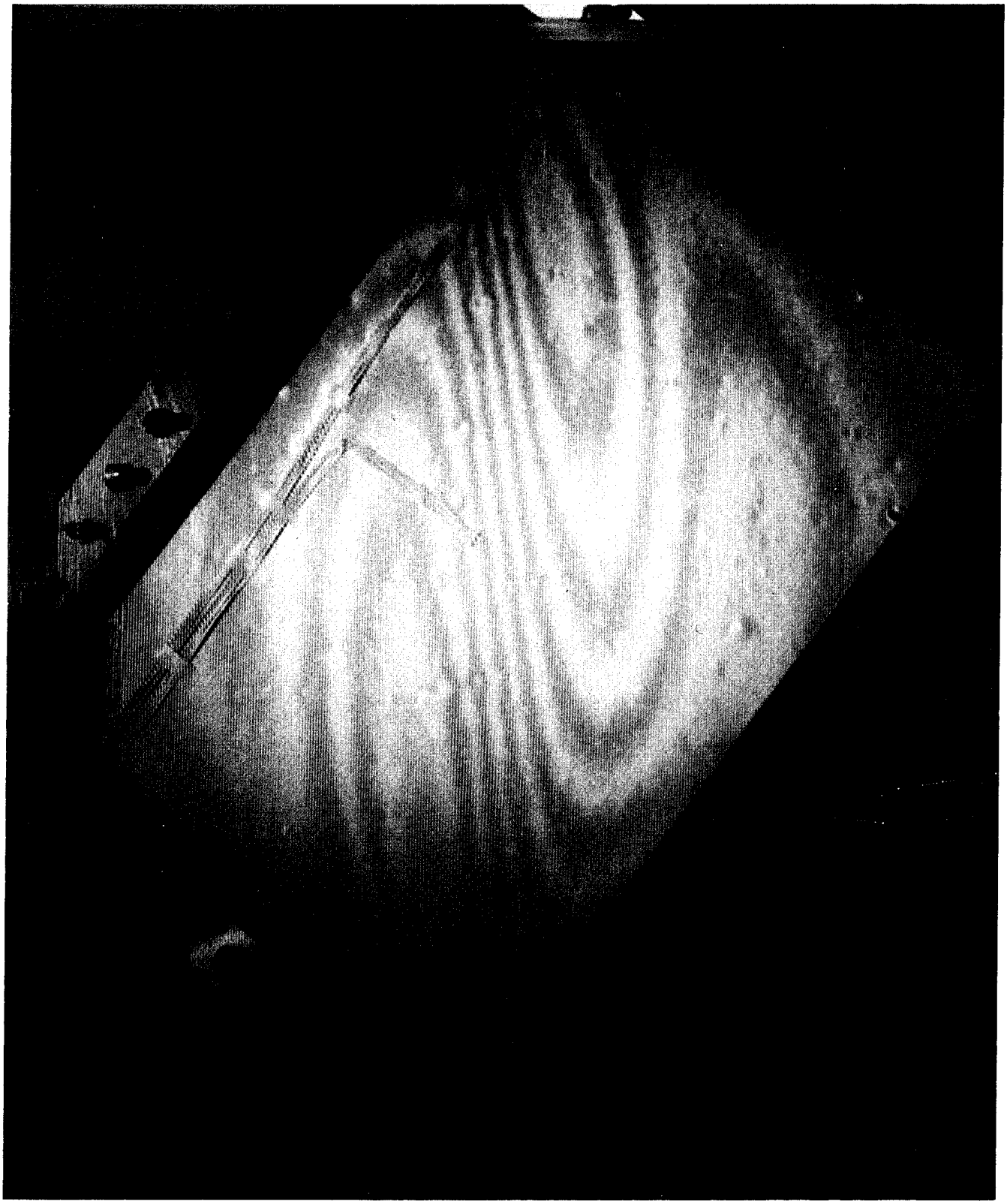

L-83-53

Figure 5.- Moiré-fringe pattern of unstiffened skin buckling mode prior to failure.

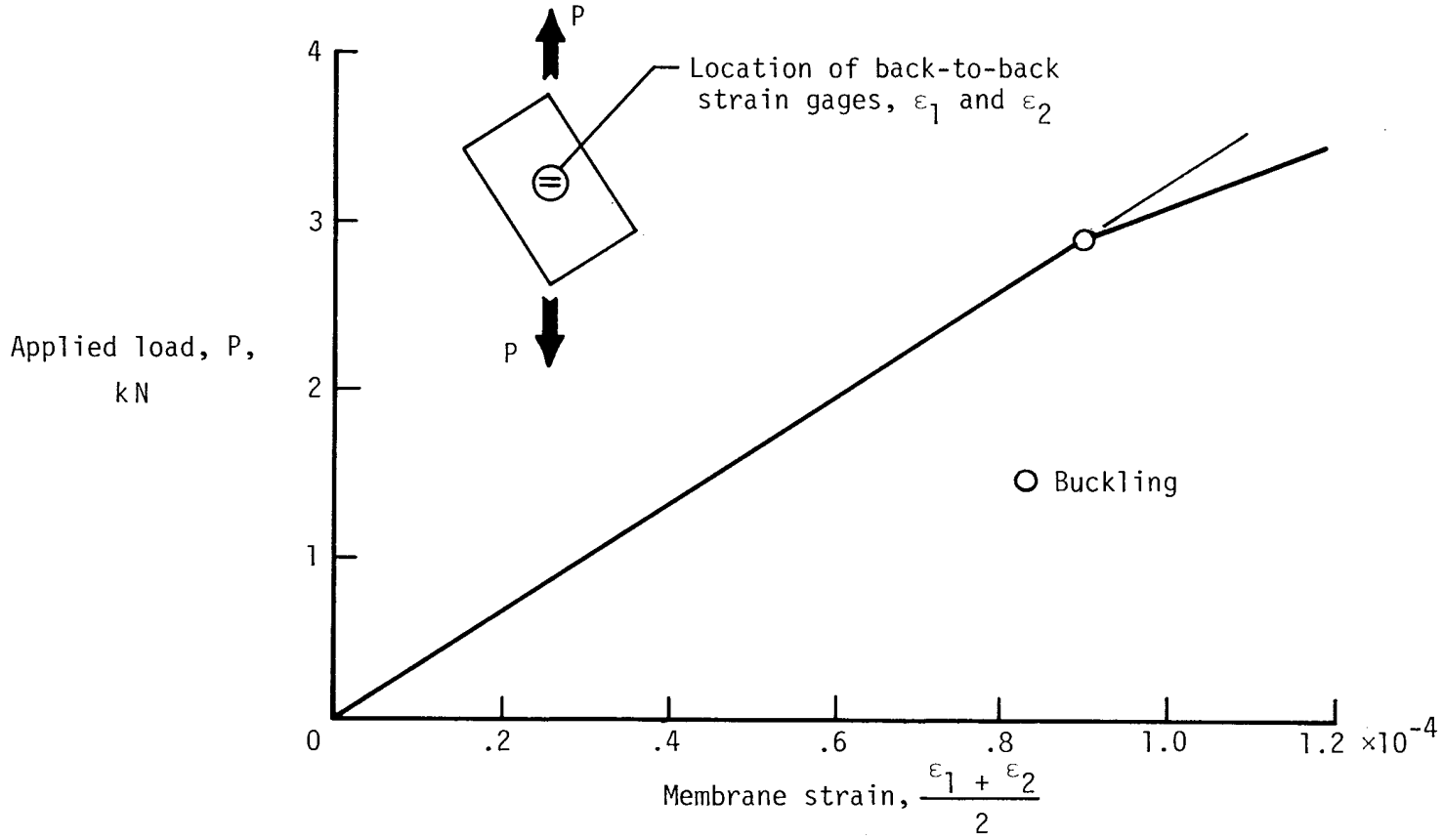

Figure 6.- Typical applied-load—membrane-strain curve for determining buckling load.

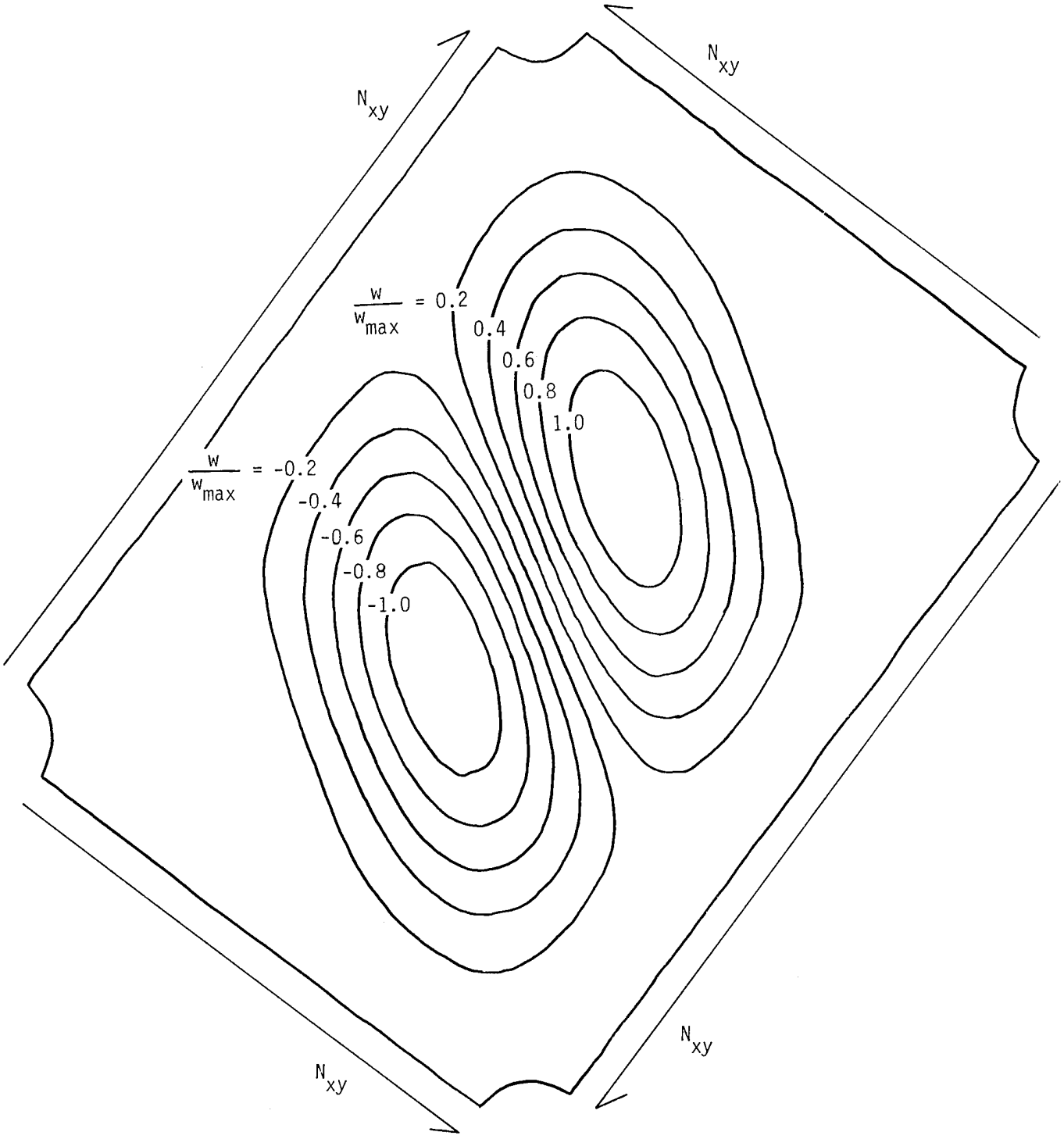

Figure 7.- Predicted normalized out-of-plane-displacement w contours for lowest buckling mode.

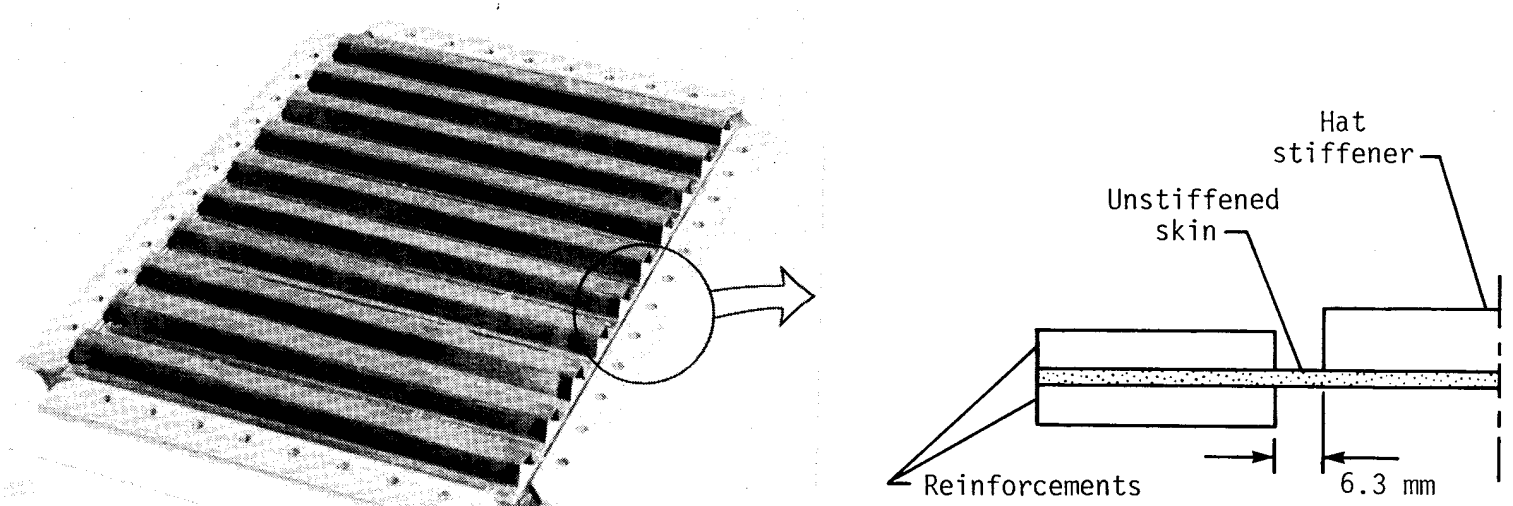

L-83-54

Figure 8.- Detail of hat-stiffened panel edge showing unstiffened skin region near reinforcements.

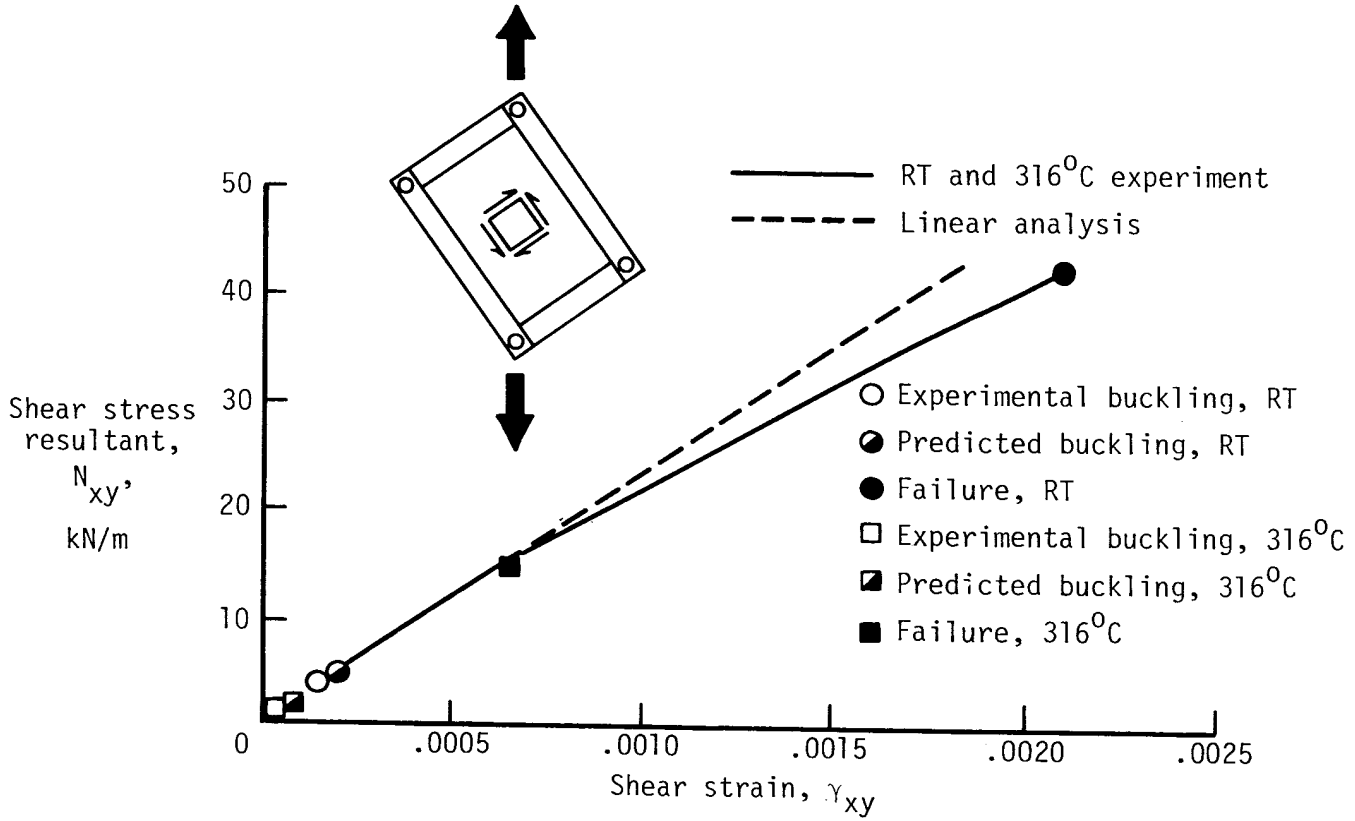

Figure 9.- Typical shear-stress-resultant—shear-strain behavior for unstiffened panels.

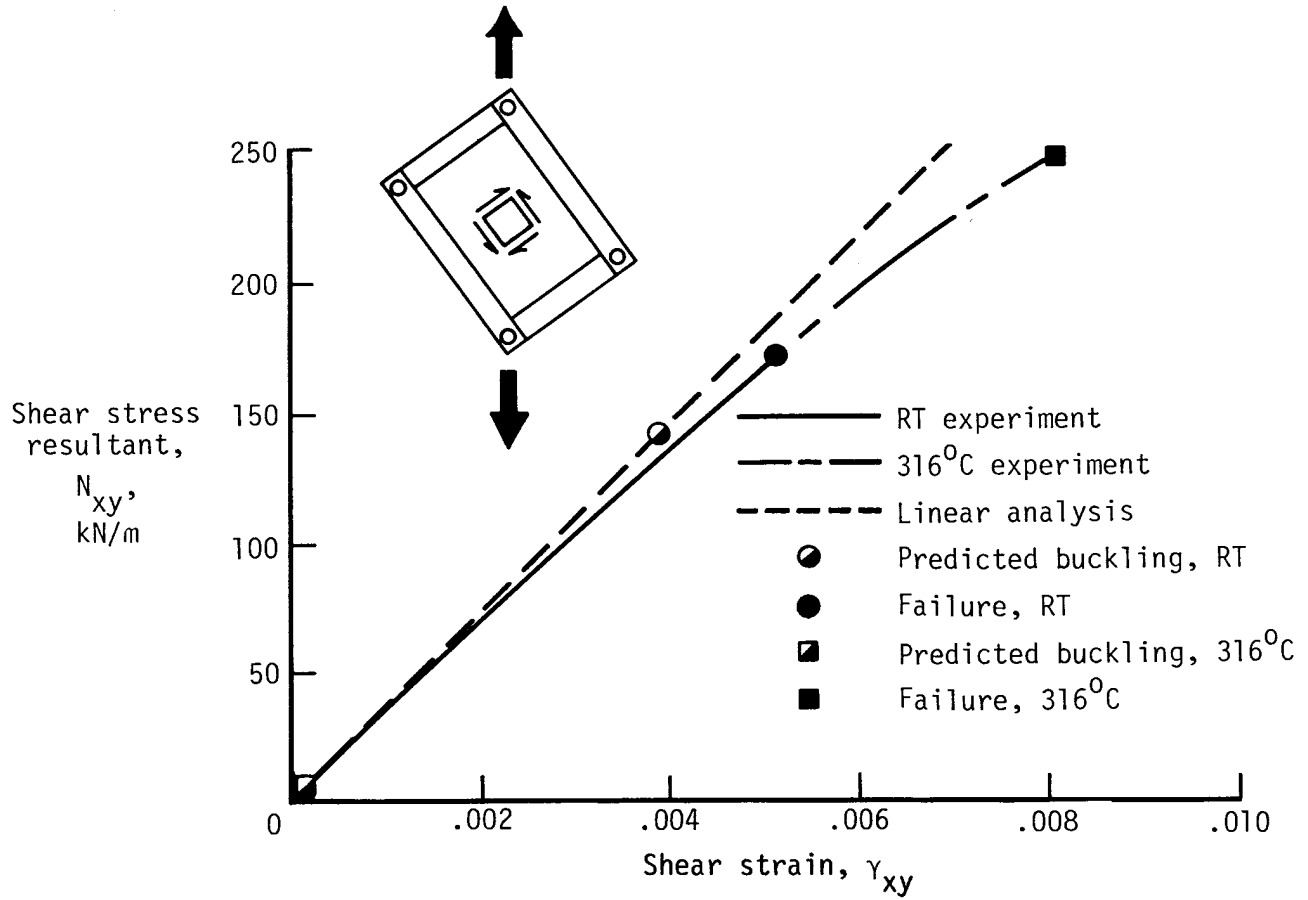

Figure 10.- Typical shear-stress-resultant—shear-strain behavior for blade-stiffened panels.

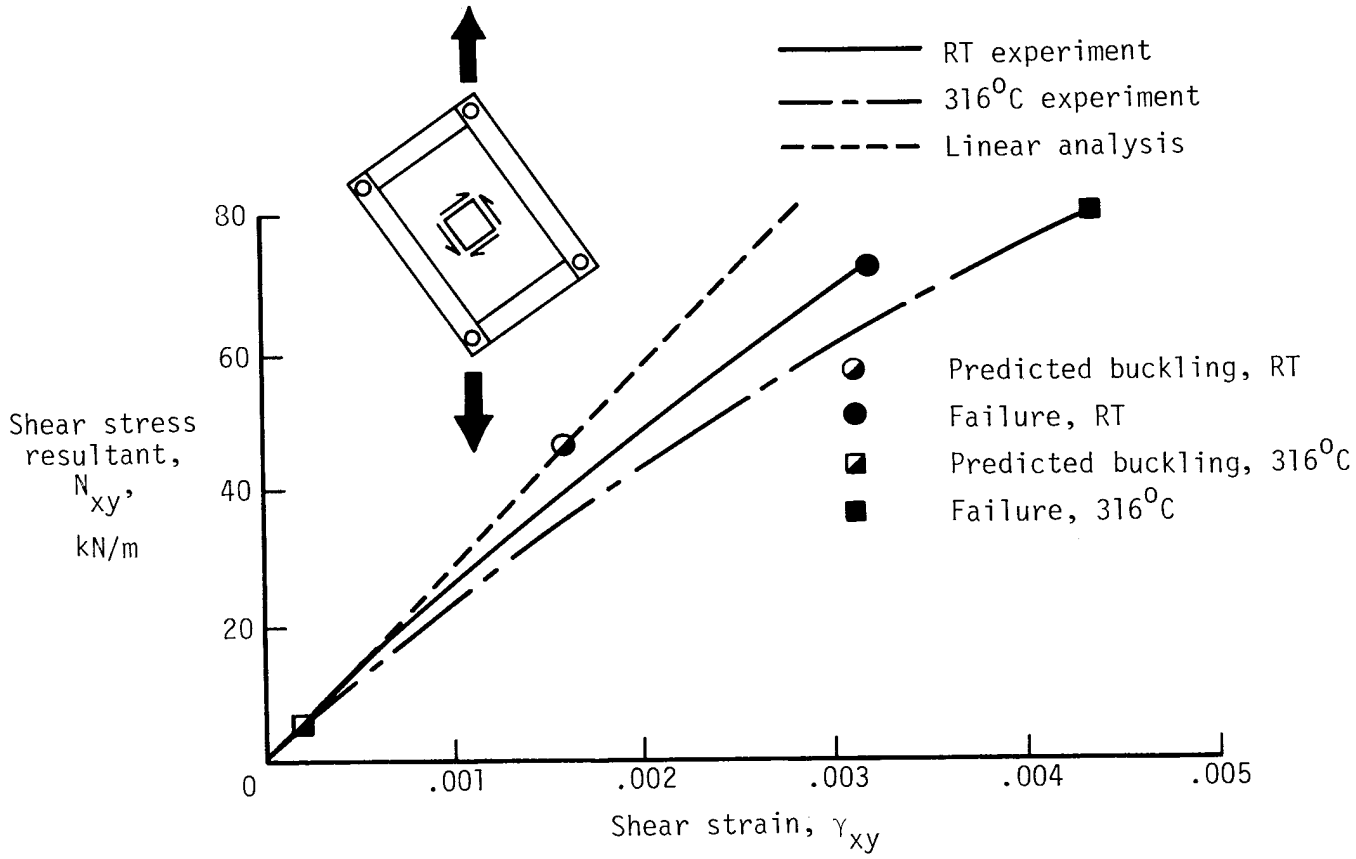

Figure 11.- Typical shear-stress-resultant—shear-strain behavior for hat-stiffened panels.

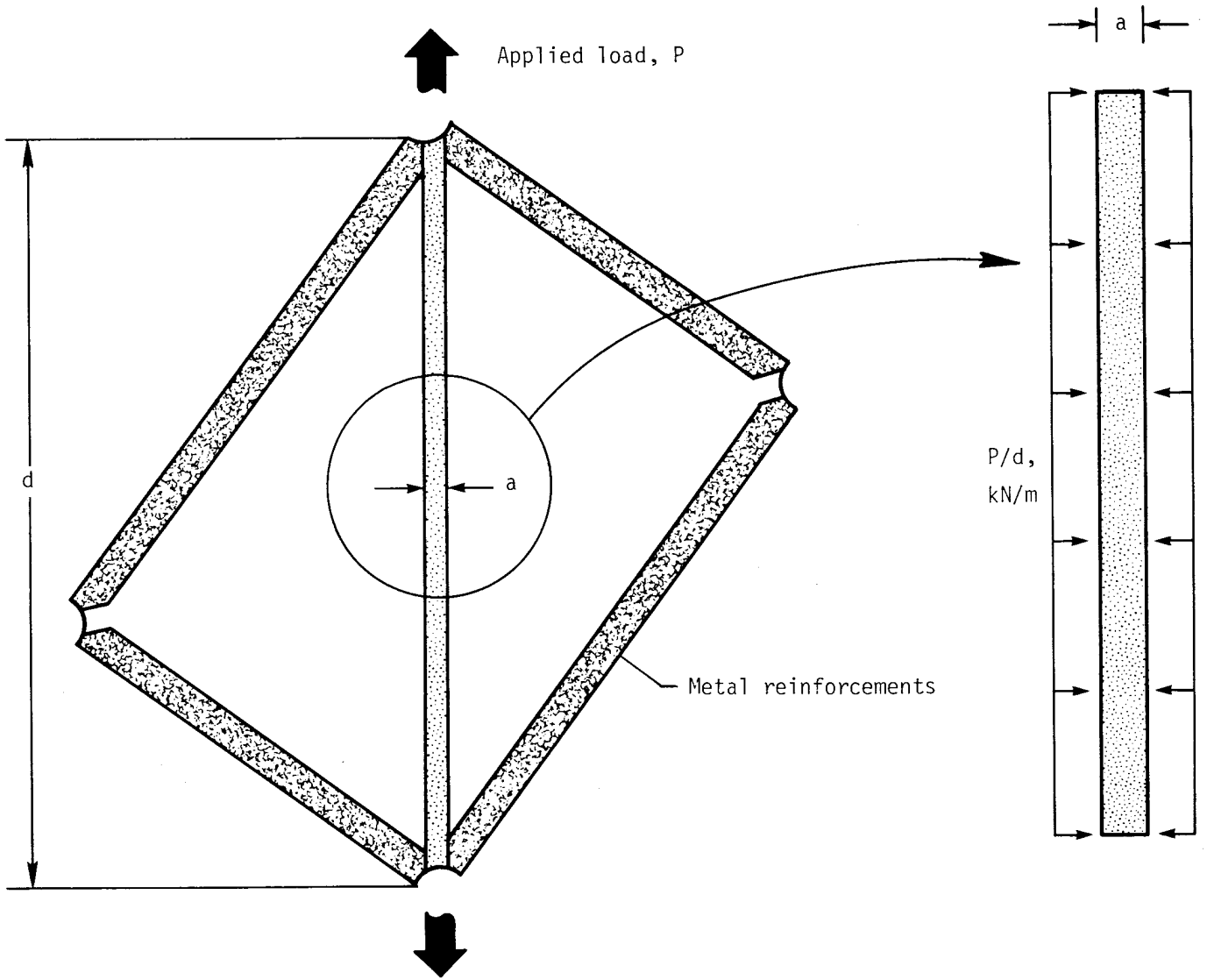

Figure 12.- Compression-loaded strip in unstiffened panels.

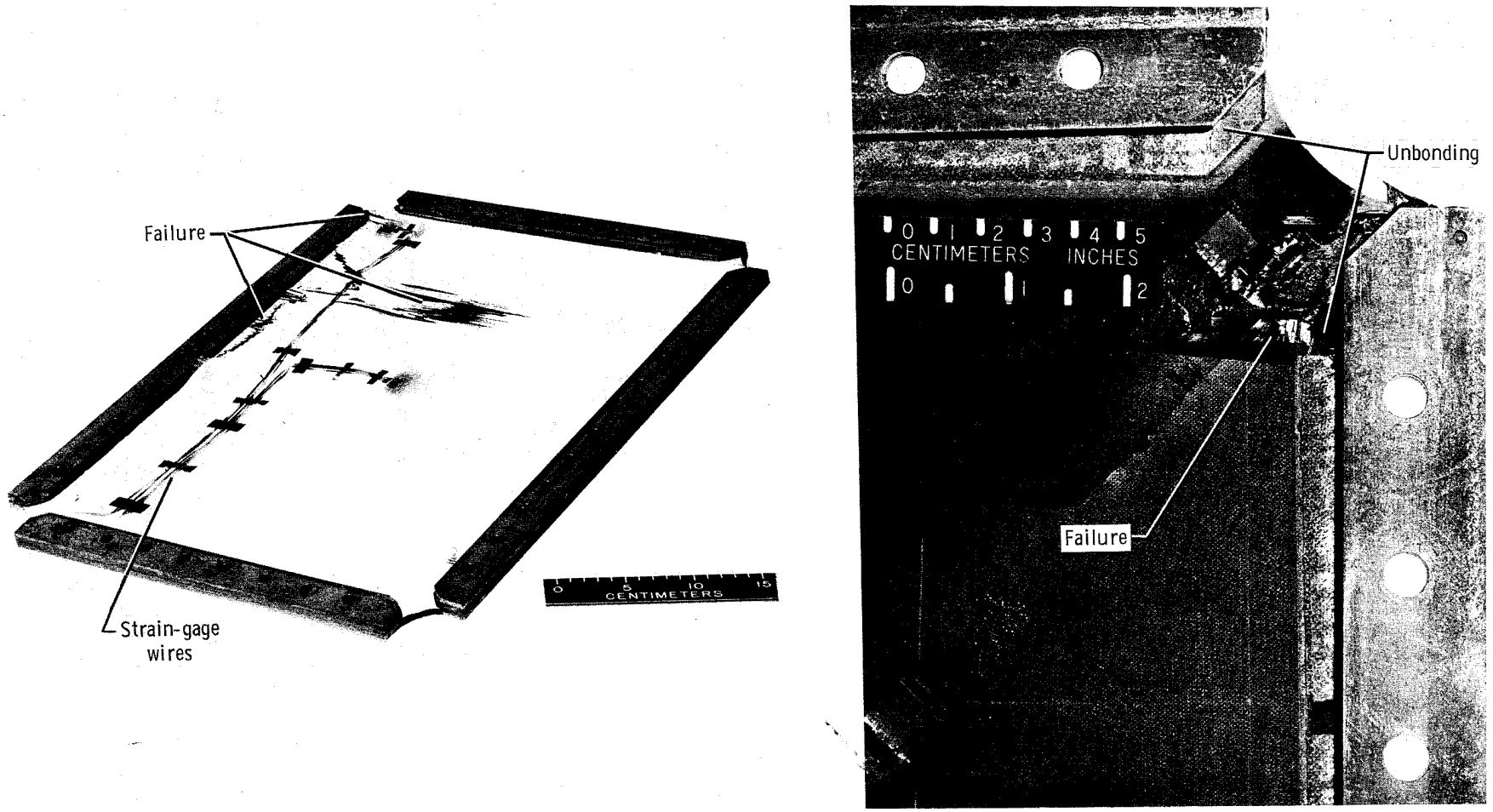

(a) Specimen tested at room temperature.

(b) Specimen tested at 316°C.

L-83-55

Figure 13.- Failed unstiffened panels.

Blade-stiffened panel

Hat-stiffened panel

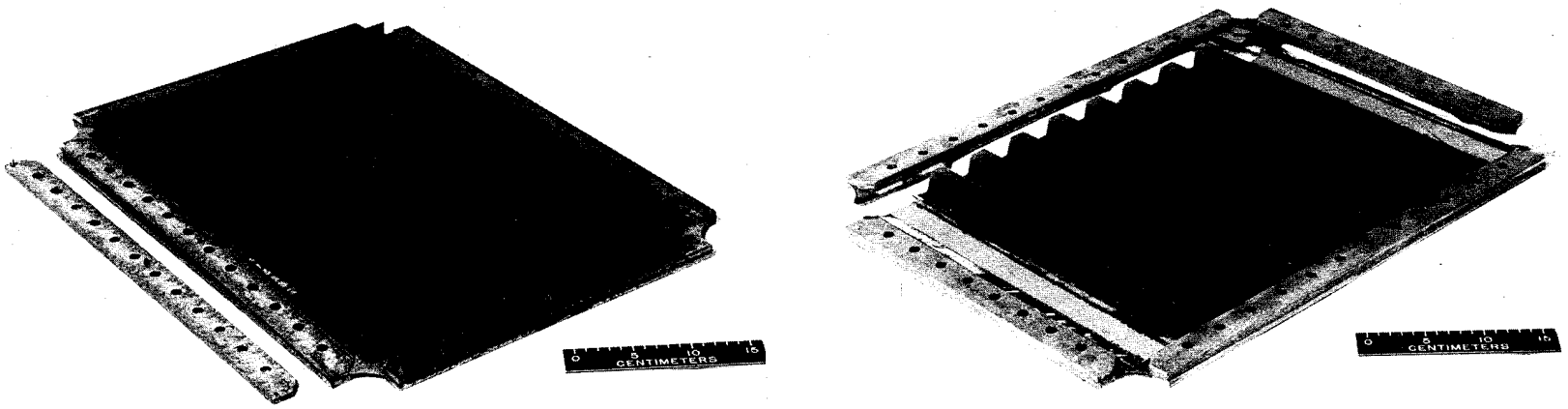

(a) Failed panels.

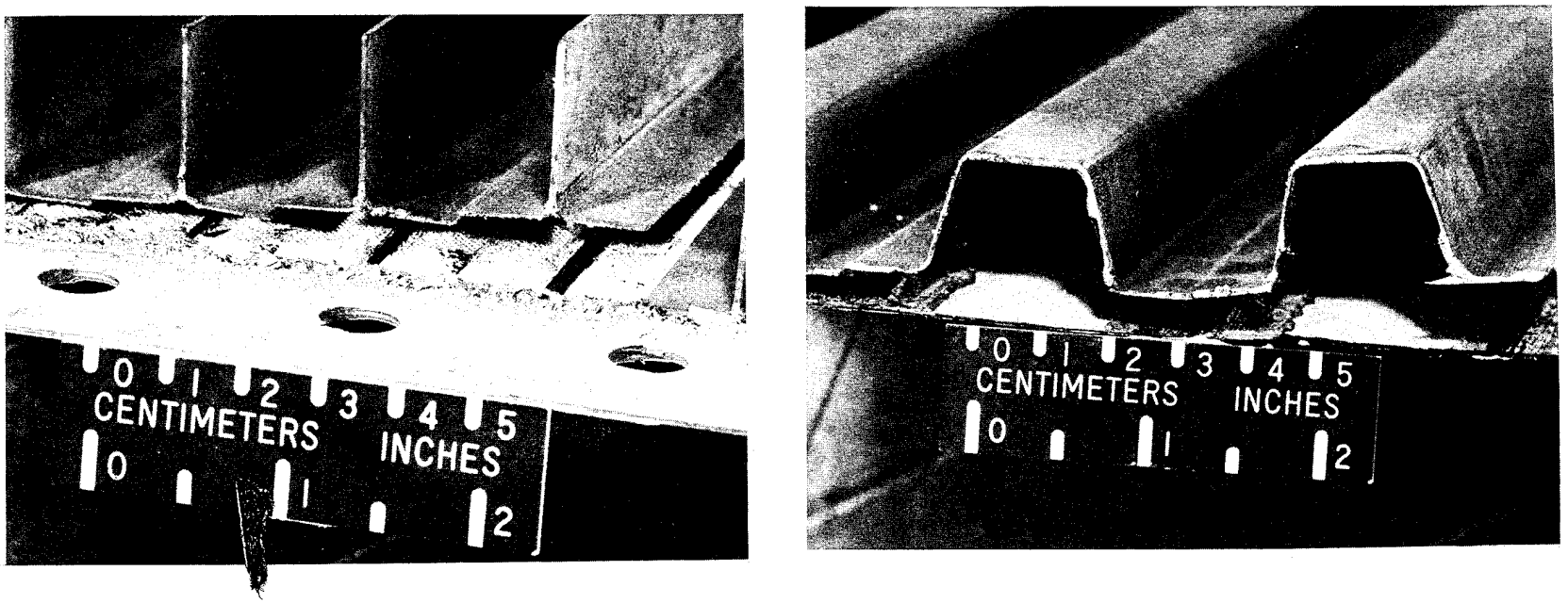

(b) Close-up view of disbonded regions.

L-83-56

Figure 14.- Failed stiffened panels.

1. Report No.	2. Government Accession No.	3. Recipient's Catalog No.
NASA TP-2153		

4. Title and Subtitle	5. Report Date
BUCKLING AND FAILURE CHARACTERISTICS OF GRAPHITE-POLYIMIDE SHEAR PANELS	May 1983
	6. Performing Organization Code 505-33-33-06
7. Author(s) Mark J. Shuart and Jane A. Hagaman	8. Performing Organization Report No. L-15557
	10. Work Unit No.
9. Performing Organization Name and Address NASA Langley Research Center Hampton, VA 23665	11. Contract or Grant No.
	13. Type of Report and Period Covered Technical Paper
12. Sponsoring Agency Name and Address National Aeronautics and Space Administration Washington, DC 20546	14. Sponsoring Agency Code

15. Supplementary Notes

16. Abstract

The buckling and failure characteristics of unstiffened, blade-stiffened, and hat-stiffened graphite-polyimide shear panels are described. The picture frame shear test is used to obtain shear stress-strain data at room temperature and at 316°C. The experimental results are compared with a linear buckling analysis, and the specimen failure modes are described. The effect of the 316°C test temperature on panel behavior are discussed.

17. Key Words (Suggested by Author(s))	18. Distribution Statement
Composite materials Graphite-polyimide laminates Shear tests Elevated temperature results Buckling behavior Failure characteristics	Unclassified - Unlimited Subject Category 24

19. Security Classif. (of this report)	20. Security Classif. (of this page)	21. No. of Pages	22. Price
Unclassified	Unclassified	23	A02

For sale by the National Technical Information Service, Springfield, Virginia 22161

NASA-Langley, 1983